



HAL
open science

THERMAL PROPERTIES OF SILICA AEROGELS

J. Fricke, E. Hümmer, H.-J. Morper, P. Scheuerpflug

► **To cite this version:**

J. Fricke, E. Hümmer, H.-J. Morper, P. Scheuerpflug. THERMAL PROPERTIES OF SILICA AEROGELS. Journal de Physique Colloques, 1989, 50 (C4), pp.C4-87-C4-97. 10.1051/jphyscol:1989414 . jpa-00229489

HAL Id: jpa-00229489

<https://hal.science/jpa-00229489>

Submitted on 4 Feb 2008

HAL is a multi-disciplinary open access archive for the deposit and dissemination of scientific research documents, whether they are published or not. The documents may come from teaching and research institutions in France or abroad, or from public or private research centers.

L'archive ouverte pluridisciplinaire **HAL**, est destinée au dépôt et à la diffusion de documents scientifiques de niveau recherche, publiés ou non, émanant des établissements d'enseignement et de recherche français ou étrangers, des laboratoires publics ou privés.

THERMAL PROPERTIES OF SILICA AEROGELS

J. FRICKE, E. HÜMMER, H.-J. MORPER and P. SCHEUERPFUG

Physikalisches Institut der Universität, Am Hubland, D-8700 Würzburg, F.R.G.

Résumé : La densité extrêmement faible des aérogels influence de manière drastique toutes les propriétés thermiques. Comparés à la silice vitreuse, les aérogels montrent une augmentation du transfert radiatif de chaleur; la conduction par le solide est réduite de deux à trois ordres de grandeurs comme cela est prédit à partir du modèle de diffusion des phonons ; aux basses températures la chaleur spécifique des aérogels est plus grande d'au moins un facteur 10 que pour le verre de silice non poreux. Le transport de chaleur dans les aérogels monolithiques et granulaires est discuté en fonction de la pression du gaz, de la température, de l'émissivité de la courbe limite et de la charge externe.

Abstract - The extremely low density of aerogels drastically influences all thermal properties: Compared to vitreous silica, aerogels show enhanced radiative heat transfer; the solid conduction is reduced by two to three orders of magnitude as can be predicted from the phonon diffusion model; at low temperatures the specific heat capacity of aerogels is larger by at least a factor of 10 than for non-porous SiO_2 -glass. Heat transport in monolithic and granular aerogels is discussed with respect to gas pressure, temperature, boundary emissivity and external load.

1 - INTRODUCTION

The steadily rising concentration of infrared active trace gases in the atmosphere, predominantly CO_2 from burning of coal, oil and natural gas, poses a severe threat to the climate on earth. Only drastic energy conservation measures and the consequent use of non-fossil energy resources may help to limit the global warming caused by a man-made atmospheric greenhouse.

In industrialised countries about 30 to 40% of the primary energy consumption is used for space heating. There is a general agreement that the long-term potential for savings in this sector is 50% or more .

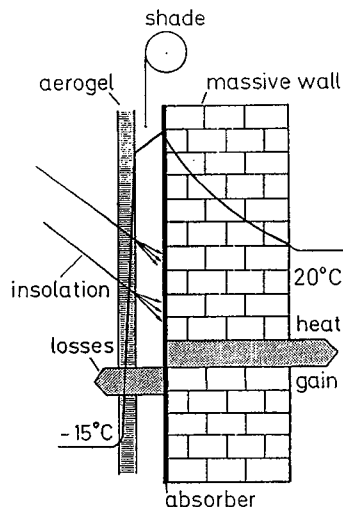


Fig.1 - Transparent house wall insulation using a superinsulating aerogel-filled glass plane system.

Promising in this respect is the development of transparent thermal insulations, which transmit solar light but effectively suppress heat transport (fig.1). A number of materials are being investigated for this purpose: capillary structures, foams, macro glass bubbles, fibers and aerogels in monolithic or granular form. Of special interest for us is the use of granular silica aerogels as transparent insulation (fig.1) in a two-family house in Ardon/Switzerland. The energy consumption for heating purposes is exceptionally low (about 300 liters of oil per year); the total investments were smaller than for a conventionally insulated house /1/. Other possible applications for aerogels are in frosted windows or in superinsulating covers for solar panels. Also solar storage collectors are being investigated, which can be operated without use of anti-freezing agents (see for example /2/).

2 - PERFORMANCE OF AN AEROGEL INSULATION

The energy flux balance for the insulations mentioned above can be estimated along the following lines /3/.

Without solar input the thermal loss coefficient k_o of the layered wall structure in fig.1 is determined by the sum of the thermal resistances R_i of its components:

$$\frac{1}{k_o} = R_o = \frac{1}{\alpha_o} + \frac{1}{\Lambda_a} + \frac{1}{\Lambda_g} + \frac{1}{\Lambda_w} + \frac{1}{\alpha_x} \quad (1)$$

$\alpha_o \approx 25 \text{ W/(m}^2\cdot\text{K)}$ and $\alpha_x \approx 8 \text{ W/(m}^2\cdot\text{K)}$ are the heat transition coefficients through the outer and inner boundary layers, respectively. Λ_a , Λ_g and Λ_w are the thermal transfer coefficients of the aerogel, the air gap and the wall, respectively.

Typical values are $\Lambda_a \approx 0.5 \text{ W/(m}^2\cdot\text{K)}$ for a 15 mm evacuated aerogel layer at 290 K, $\Lambda_g \approx 6 \text{ W/(m}^2\cdot\text{K)}$ for a 1 cm wide air gap and $\Lambda_w \approx 1 \text{ W/(m}^2\cdot\text{K)}$ for a massive 25 cm thick wall. We end up with a thermal loss coefficient $k_o \approx 0.3 \text{ W/(m}^2\cdot\text{K)}$.

If we now take into account that the black wall absorbs part of the solar flux and that the thermal losses thus are partially compensated, we may describe the system with an effective loss coefficient

$$k_{eff} = k_o - q_{s01} \cdot t \cdot \eta / \Delta T. \quad (2)$$

$q_{s01} \cdot t$ is the solar flux, which is transmitted through the aerogel insulation of transmissivity t and impinges onto the wall. For simplicity we assume q_{s01} to be constant in time. ΔT is the mean difference between the temperatures inside and outside the house, T_i and T_e , respectively. η is an efficiency, equivalent to the fraction of the solar flux which is absorbed and transferred into the house. The quantity $q_{s01}/\Delta T$ in equ.2 is given by the climatic conditions while k_o , t and η can be chosen according to the technical design. If we introduce the solar gain coefficient

$$k_{s01} = q_{s01} / \Delta T, \quad (3)$$

equ.2 can be rewritten as

$$k_{eff} = k_o - k_{s01} \cdot \eta t. \quad (4)$$

The plot of k_{eff} versus k_{s01} is a straight line with a negative slope, equal to ηt . the thermal losses from the interior to the environment vanish for

$$k_{s01,0} = k_o / \eta t. \quad (5)$$

Let us assume that the total transmitted solar flux $q_{s01} \cdot t$ is absorbed at the outer surface of the wall. If no net heat flux is to be transferred into or out of the house, the temperature of the absorbing layer has to be equal to T_i , the temperature of the interior. Thermal losses then are determined by the resistances of the aerogel layer and the air gap. (α_o is assumed to be infinitely large.) The flux balance then becomes

$$\Delta T \cdot (1/\Lambda_a + 1/\Lambda_g)^{-1} = q_{s01,0} \cdot t, \quad (6)$$

or with equ.3, $\Lambda_o \gg \Lambda_a$ and $t = 0.6$

$$k_{s01,0} \approx \Lambda_a / t \approx 0.8 \text{ W/(m}^2\cdot\text{K)}. \quad (7)$$

Thus under steady state conditions (which, admittedly, are not very realistic) a solar flux per temperature difference $q_{sol}/\Delta T = k_{sol,o} = 0.8 \text{ W}/(\text{m}^2 \cdot \text{K})$ is necessary to thermally decouple the interior of the house from the environment.

This value for aerogel layers is lower than for other transparent insulations (table 1).

		typical thickness cm	Λ W/m ² ·K	diffuse transm. %	$k_{sol,o}$ / W/m ² ·K
SiO ₂ - aerogel tiles	in air	1.5	1	60	1.6
	evacuated	1.5	0.5	60	0.8
granular SiO ₂ - aerogel	in air	1.5	1	50	2
	evacuated	1.5	0.5	50	1
Arel capillary structure, polycarbonate (incl. gap)		10	0.9	60	1.5
fiber layers, D = 20 μm (incl. gap)		5	1.2	40	3
macro glass bubbles D = 3...5 mm		2	2	50	4

Table 1 - Comparison between various transparent insulation systems

3 - THERMAL TRANSPORT IN MONOLITHIC AEROGELS

All thermal applications of silica aerogels require precise information on the heat transfer, which proceeds via infrared (IR) radiation and solid conduction. SiO₂ aerogels in layers of 1 to 2 cm are not optically thick and therefore heat transfer is a complex phenomenon in this material.

3.1 - RADIATIVE HEAT TRANSFER

IR extinction is provided by absorption. The absorption in aerogel is strong above wavelength of 7 μm, however especially low between 3 and 5 μm (fig.2). Therefore at low temperatures (280 K), the thermal IR transmission spectrum is effectively attenuated, and the radiative transport through aerogel is weak. For increasing temperatures, however, more and more radiation can penetrate the material within the wavelengths range 3-5 μm (fig.3). Silica aerogel then gradually loses its insulating properties.

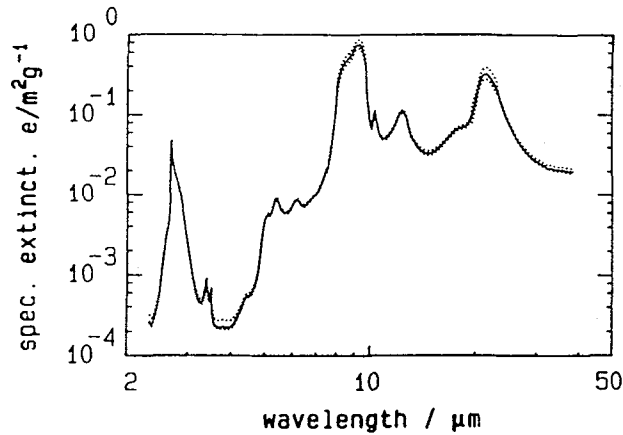


Fig.2 - Specific extinction coefficient $e=E/\rho$ for silica aerogel on a logarithmic scale versus wavelength; the strong absorption bands at 9.5, 12.5 and 21 μm also are observed for silica glass; the 2.7 μm absorption band is caused by vibrations of the OH- Groups bound to Si-atoms /4/.

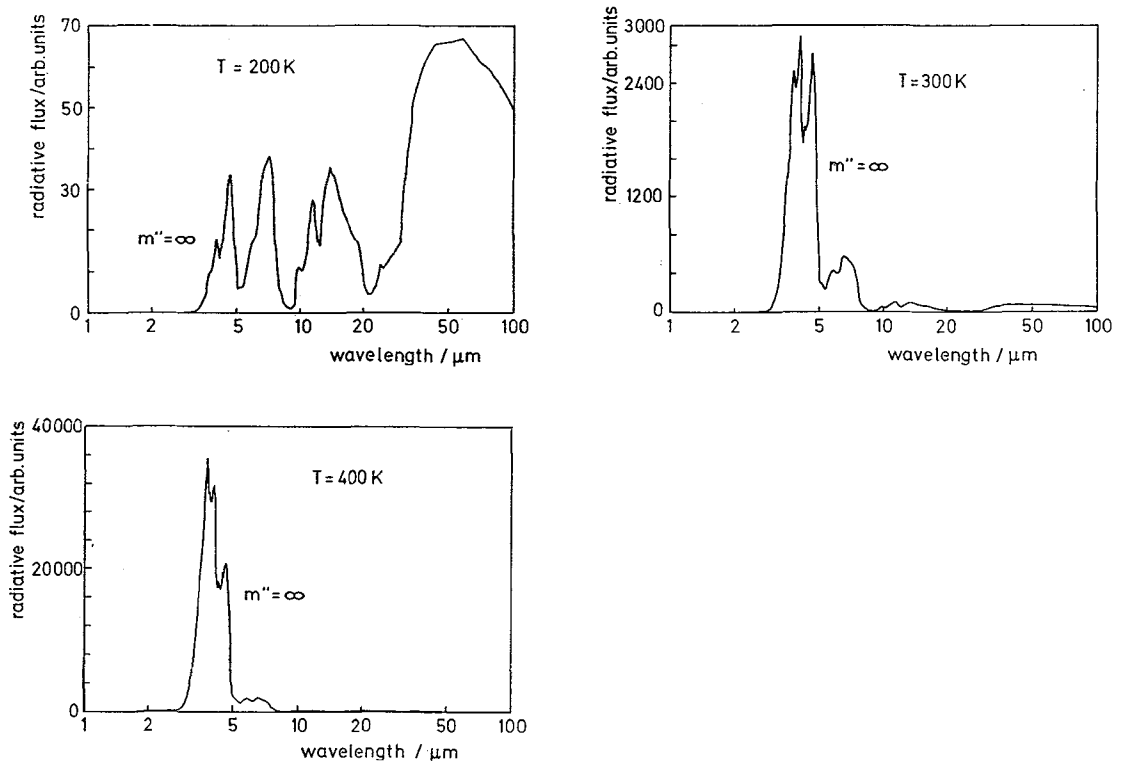


Fig.3 - Relative spectral flux through silica aerogel between black boundaries for $T_x = 200, 300,$ and 400 K /5/; note the different ordinate scales. For $T_x = 200\text{ K}$ the major radiative contribution occurs above wavelenghts of $50\ \mu\text{m}$; low boundaries would cut off the flux maxima.

3.2 - SOLID CONDUCTION

The tenuous structure is expected to provide a drastically reduced solid conductivity compared to silica glass. From the phonon diffusion model for non-porous SiO₂ glass (index G) and for aerogels (index A)

$$\lambda_G = c_{v,G} \cdot \ell_G \cdot \rho_G \cdot v_G / 3$$

$$\lambda_A = c_{v,A} \cdot \ell_A \cdot \rho_A \cdot v_A / 3$$
(8)

we derive the following equation

$$\lambda_A \approx \lambda_G \cdot (\rho_A/\rho_G) \cdot (v_A/v_G).$$
(9)

Both the phonon mean free paths ℓ in SiO₂ glass and in aerogels are expected to be in the order of 1 nm. The specific heat capacities c_v for both materials differ markedly below 10 K /6,7/; At elevated temperatures the c_v values for glass and for aerogel are comparable. For an estimate we consider an aerogel with density $\rho_A = 100 \text{ kg/m}^3$ and equate the phonon group velocity with the sound velocity $v_A \approx 100 \text{ m/s}$ derived from ultrasonic measurements /8/. For $T = 300 \text{ K}$, where $\lambda_G \approx 1.3 \text{ W/(m}\cdot\text{K)}$ we then get $\lambda_A = 1.3 \text{ W/(m}\cdot\text{K)} \cdot (100/2200) \cdot (100/5000) \approx 10^{-3} \text{ W/(m}\cdot\text{K)}$, a value which is, to our knowledge, by far the lowest ever reported for a solid material. We want to mention that we have successfully tested the validity of the phonon diffusion model at room temperature for compressed powders over a large density range /9/. Recent measurements on the solid thermal conductivity of aerogels are presented in fig.4. Our data have been collected from stationary measurements with two "hot plate" systems, one cooled with LN₂ /10/, the other with LHe.

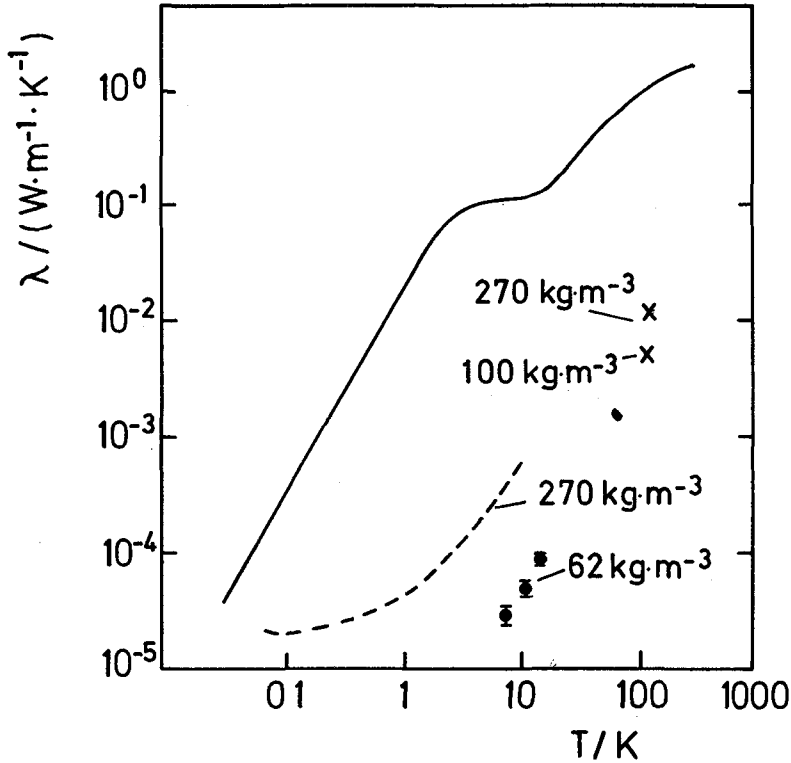


Fig.4 - Double log plot of thermal conductivity versus temperature for non-porous silica glass and aerogels ($\rho=270, 100$ and 62 kg/m^3);
 (—) Zeller and Pohl /10/, (---) Calemczuk et.al. /6/, (x) Heinemann et.al. /11/,
 (•) data from our "hot plate" cryogenic system.

We recognize that the solid thermal conductivity dramatically varies with density, as predicted. The values for various densities differ (by a factor of 500 or so for the 100 kg/m³ aerogel) between room temperature and about 4 Kelvin.

3.3. - COMBINED RADIATIVE AND CONDUCTIVE HEAT TRANSFER

For optically thick insulations, for example opacified fiber or powder systems, the solid and the radiative conductivities λ_{sc} and λ_r , respectively, are well defined and are linearly superposed:

$$\lambda = \lambda_{sc} + \lambda_r, \quad (10)$$

with

$$\lambda_r = (16 \cdot n^2 \cdot \sigma \cdot T_r^3) / (3 \cdot e \cdot \rho) \quad (11)$$

$$T_r = \{(T_1^2 + T_2^2) \cdot (T_1 + T_2)\}^{1/3} \quad (12)$$

$e = E/\rho$ is the specific extinction coefficient, σ the Stefan Boltzmann constant and n the average index of refraction of the insulation. T_1 and T_2 are the boundary temperatures. As λ_{sc} is only weakly dependent on temperature equations (10) and (11) may be displayed in a simplified λ versus T_r^3 diagramm (see fig.5).

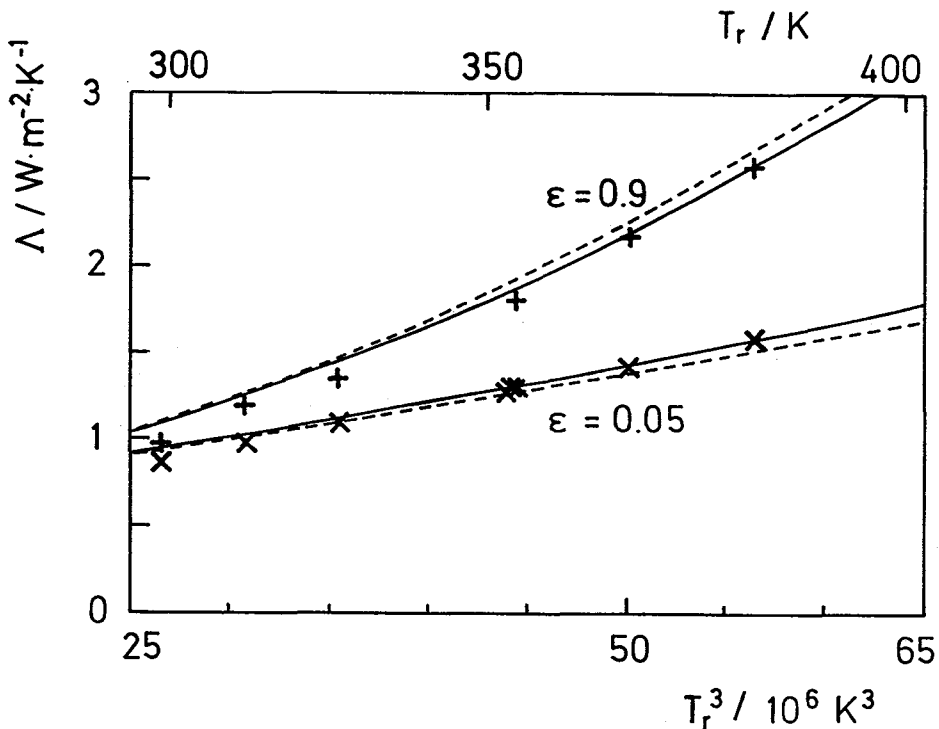


Fig.5 - Thermal conductivity for an specially thick insulation; the data are load bearing fiber insulation /12/.

For optically thin, non-conducting gray insulations the radiative flux can be estimated from

$$q_r = (n^2 \cdot \sigma \cdot (T_1^4 - T_2^4)) / (2/\epsilon - 1 + 3/4 \cdot \tau_o). \quad (13)$$

with $\tau_o = E \cdot d$. This equation will give wrong results in the general case of non-zero solid conduction and low boundary emissivities ($\epsilon \ll 1$). Then a considerable amount of radiation emerges from the radiative boundary layers close to wall (fig.6).

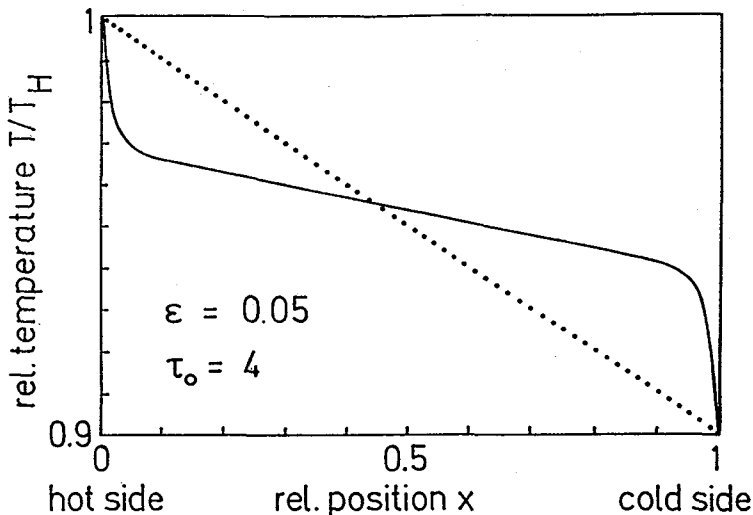


Fig.6 - Temperature profile for pure conduction (dotted line) and for a medium with a radiative boundary layer.

Due to the strong temperature gradient near the wall the energy can effectively be delivered into the boundary layers via solid conduction. The amount of radiation emitted from the boundary layers depends on its optical absorption thickness τ_o . Furthermore, the lower the emissivity ϵ of the walls for a given τ_o the more radiation, compared to the emission of the walls, will proceed from the boundary layers into the aerogel tile. To take care of the boundary-layer effect the emissivity ϵ in equation (13) may be substituted by a (higher) effective emissivity /13/

$$\epsilon' = 1 - (1-\epsilon) \cdot \exp[-\arctan(\tau_o)/2]. \tag{14}$$

In general the combined radiative and conductive heat transfer is described by an integro-differential equation. It is tedious to solve the exact equation numerically for a non-gray medium as aerogel, where the optical thickness τ_o is a function of wavelength. However, it is possible to work with a generalized three-flux equation, presented for gray media /14/ (see fig.7).

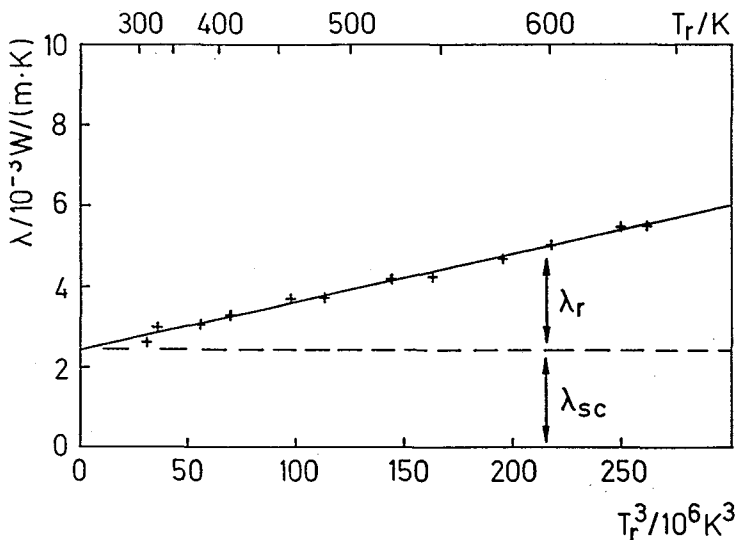


Fig 7 - Thermal transfer coefficient for an aerogel like ($\rho=77 \text{ kg/m}^3$, $d=9 \text{ mm}$) as a function of mean temperature T_r ; (+) measurements, (—) numerical solution of general heat transfer equation, (---) approximate spectral three-flux equation.

3.4. - INFLUENCE OF GAS PRESSURE

The structural build-up in aerogel occurs in the 1 to 100 nm range, which is known from light scattering, SAXS, SANS and BET measurements. Therefore gas conduction is not expected to be fully developed in aerogels, even at pressures of 1 bar. The thermal conduction under variation of gas pressure and its correlation with structure was extensively studied by S.S.Kistler about 50 years ago /15/. Recent measurements /16/ show, that for 80 kg/m³ aerogels the gas-induced rise of thermal losses only occur for pressures above 50 mbar (see fig.8). The derived average size for the "pores" is about 100 nm.

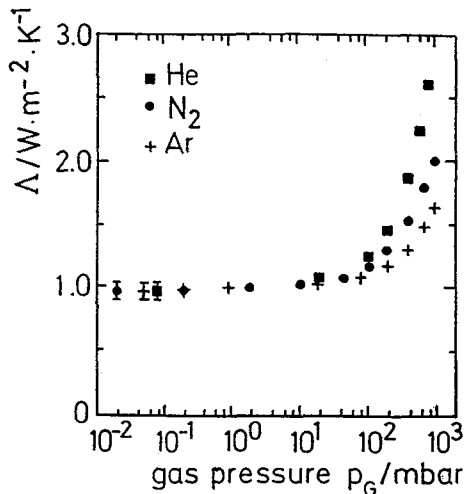


Fig.8 - Thermal transfer coefficient for a 80 kg/m³ aerogel tile of 9 mm thickness versus gas pressure; the mean temperature was T_r=300 K.

4. - THERMAL TRANSPORT IN GRANULAR AEROGELS

Though S.S.Kistler has produced and investigated granular silica aerogels, only today large enough quantities of this material are available for detailed investigations of thermal and other properties. The granular material currently available is produced from water glass and has a density of about 200 to 250 kg/m³ /17/. It thus has the potential for large scale applications in passive solar usage /1/.

4.1 - RADIATIVE HEAT TRANSFER

As infrared scattering in granular fills can be neglected the specific extinction coefficients resulting from absorption are expected to be comparable to those of monolithic specimens.

4.2 - SOLID CONDUCTION

The thermal resistance of the many point contacts in granular and powderous fills can be treated according to the Kaganer model /18/. The resulting solid conductivity is

$$\lambda_{sc} = \lambda_s \left[\frac{12}{\pi^2} \cdot (1 - \mu_s^2) \cdot (1 - \Pi)^2 \exp(4.8 \cdot (1 - \Pi)) \cdot p_{ext} / Y_s \right]^{1/3}. \quad (15)$$

For $\rho_s = 230$ kg/m³, $\Pi = 0.34$, $Y_s = 10^7$ N/m², $\mu_s = 0.2$, $p_{ext} = 10^5$ N/m² we get $\lambda_{sc} \approx 0.5 \lambda_s$. In general one thus expects loaded (1 bar) granular fills to have half the solid conduction as monolithic layers.

4.3 - MEASUREMENTS ON EVACUATED GRANULAR FILLS

Thermal conductivity measurements on evacuated granular aerogel layers have been performed over a temperature range from 0 to 350 °C. The tested specimen consisted of sifted pellets with diameters between 1 to 2 mm. The boundary emissivity was $\epsilon = 0.04$, the external load $p_{ext} = 0.1$ bar. Surprisingly the measured temperature dependence is linear in T_r⁻³ (fig.9). This could falsely be interpreted as resulting from a temperature independent extinction coefficient in an optically thick specimen. The proper interpretation, however, is that in

aerogels the extinction coefficient markedly decreases with rising temperature. This has two consequences. Firstly the radiative boundary layer effect, discussed above, gets weaker with increasing temperature. Secondly radiation emerging from the boundary layer is attenuated less at higher temperatures. Obviously the two effects just happen to produce the result of fig.9. In addition it is helpful to compare the measured transfer coefficient with the case

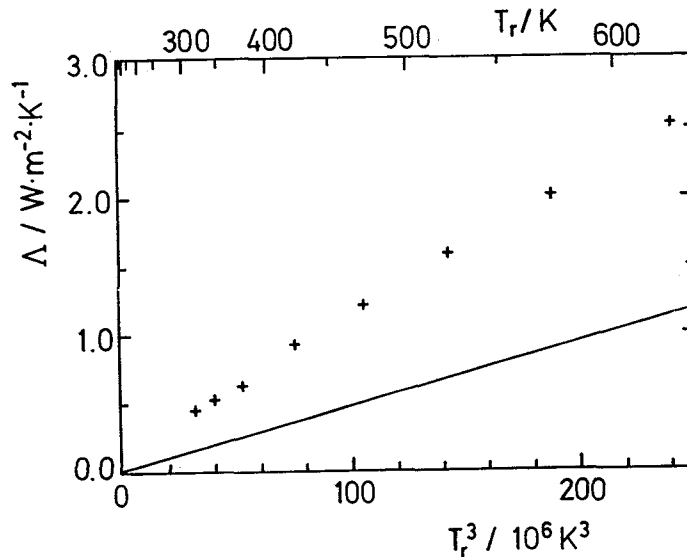


Fig.9 - Thermal transfer coefficient Δ versus T_r^3 for an evacuated 24 mm thick granular aerogel layer with external load $p_{ext} = 0.1$ bar; the boundary emissivity is $\epsilon = 0.04$; the mass per area 3.18 kg/m^2 . For comparison the transfer coefficient for an evacuated spacing with $\tau_o = 0$ is shown.

of an evacuated empty spacing. The straight line in fig.9 calculated for $\epsilon = 0.04$ shows that thermal transport in this case is weaker, indicating that the aerogel layer roughly doubles the heat transfer.

The dependence of the thermal transfer coefficient from external load is shown in fig.10. While below $p_{ext} \approx 0.2$ bar the rise is quite steep, the increase for higher loads is remarkably weak. The qualitative interpretation is that the steep rise is caused by an increase of solid conduction combined with an enhancement of the radiative boundary layer.

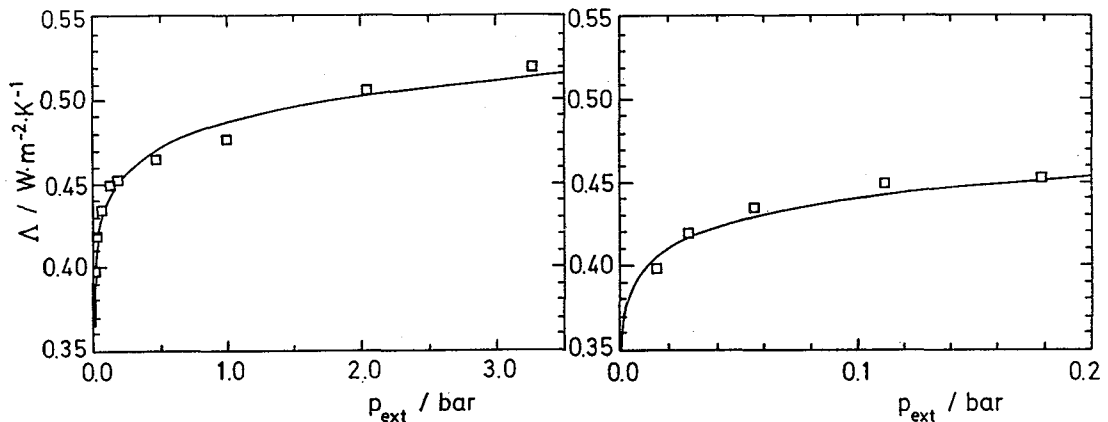


Fig.10 - Thermal transfer coefficient Δ versus p_{ext} for an evacuated granular aerogel layer with the same mass per area as in fig.9; the average temperature is $T_r = 318 \text{ K}$; the fit was performed according to the relation $\Delta = \Delta_o + \text{const.} \cdot (p_{ext}/\text{bar})^\beta$, with $\Delta_o = 0.15 \text{ W} \cdot \text{m}^{-2} \cdot \text{K}^{-1}$, $\text{const.} = 0.34 \text{ W} \cdot \text{m}^{-2} \cdot \text{K}^{-1}$, $\beta \approx 1/15$; fig.10a displays a wide load range; in fig.10b the steep increase in Δ up to $p_{ext} = 0.2$ bar is shown.

4.4 - EFFECTS OF GAS PRESSURE

The gas pressure dependence of the apparent thermal conductivity shown in fig.11 displays the two-step picture expected for porous materials with two distinctly different pore sizes. The fit curve represents a behaviour

$$\lambda(p_{\text{GAS}}) = \lambda_0 + \lambda_1/(1+p_1/p_{\text{GAS}}) + \lambda_2/(1+p_2/p_{\text{GAS}}), \quad (16)$$

where $\lambda_0 = 10.3 \cdot 10^{-3} \text{ W/(m}\cdot\text{K)}$ is the conductivity for an evacuated fill, $\lambda_1 = 7.6 \cdot 10^{-3} \text{ W/(m}\cdot\text{K)}$ represents the low pressure increase in conductivity caused by the space between the pellets and $\lambda_2 = 9.5 \cdot 10^{-3} \text{ W/(m}\cdot\text{K)}$ the high pressure increase of λ caused by the pores within the pellets. $p_1 \approx 0.09 \text{ mbar}$ and $p_2 \approx 1050 \text{ mbar}$ are the pressures where $\lambda_1/2$ and $\lambda_2/2$, respectively, are reached.

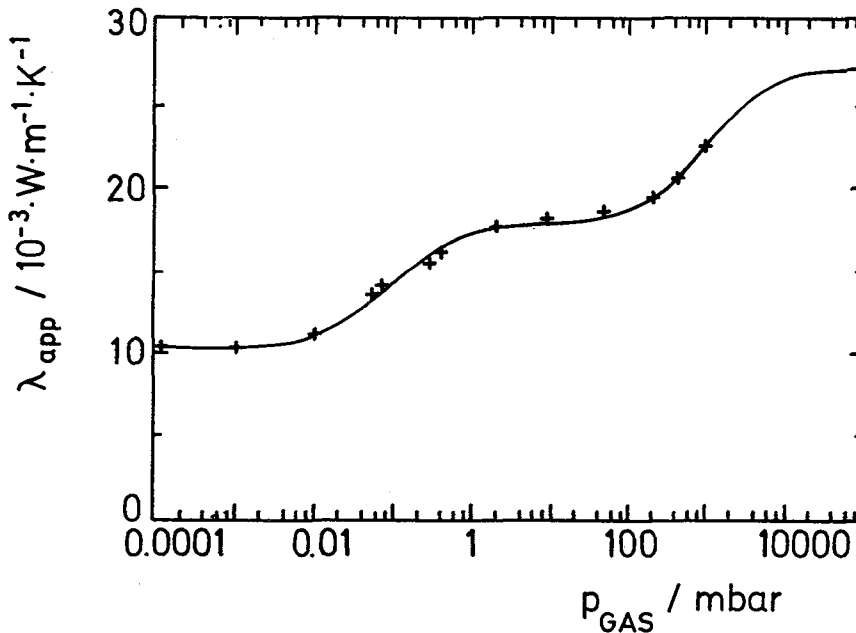


Fig.11 - Measurements and fit curve for apparent total thermal conductivity λ_{app} versus gas pressure p_{GAS} for the same granular fill as in fig.9; the mean temperature is $T_r \approx 318 \text{ K}$.

5 - OUTLOOK

The presented conductivity data show that there is in general a good understanding of the thermal transport in monolithic and granular aerogel systems. Of special interest to solid state physicists is the low temperature conductivity - a field which certainly needs further research. A difficult problem is the extraction of the solid conductivity from measured values at elevated temperatures, where radiation cannot be neglected.

Acknowledgements

This work was supported by the German Bundesminister für Forschung und Technologie.

REFERENCES

- /1/ Novakov, Report on the Cité Solaire, Ardon/Switzerland at the 2nd International Workshop on Transparent Insulation, Freiburg March 1988

- /2/ Schmidt, Ch., Goetzberger, A. and Schmid, J., Test Results and Optimization of Integrated Collector Storage with a Transparent Insulating Cover, 2nd International Workshop on Transparent Insulation
- /3/ 10th Symposium on Thermophysical Properties, Gaithersburg/Maryland, June 1988 'Fibrous Insulations with Transparent Cover for Passive Use of Solar Energy'
- /4/ Döll, G., 'Wärmetransport durch nicht-graue optisch dünne Medien', Diplom Thesis Univ. of Würzburg, Report E12-0987-3 (1987)
- /5/ Caps, R., Private Communication
- /6/ Calemczuk, R., De Goer, A.M., Salce, B., Maynard, R., and Zarembowitch, A., Europhys.Lett. 3, 1205 (1987)
- /7/ Reichenauer, G., Fricke, J., and Buchenau, U., Neutron Scattering Study of low Frequency Vibrations in Silica Aerogels, Report E21-0788-1 (1988) submitted to Europhysics Letters
- /8/ Gronauer, M., Kadur, A., Fricke, J., Mechanical and Acoustical Properties of Silica Aerogels in 'Aerogels' Springer Proceedings in Physics 6, J. Fricke (Ed), Springer Verlag Berlin 1986
- /9/ Nilsson, O., Rüschenpöhler, G., Groß, J., and Fricke, J., Compressed Porous Media - Correlation between Thermal Conductivity and Elasto-Mechanical Properties, 11th European Conference on Thermophysical Properties, Umea/Sweden, June 1988
- /10/ Zeller and Pohl, Phys. Rev. B4, 2029 (1971)
- /11/ Heinemann, U., Hümmer, E., Büttner, D., Caps, R., Fricke, J., High Temp.-High Press. 18, 517 (1986)
- /12/ Caps, R., Trunzer, A., Büttner, D., Fricke, J., Int. J. Heat Mass Transfer 27, 1865
- /13/ Scheuerpflug, P., Caps, R., Büttner, D. and Fricke, J., Int. J. Heat Mass Transfer 28, 2299 (1985)
- /14/ Fricke, J., Caps, R., Heat Transfer in Thermal Insulations - Recent Progress in Analysis, 10th Symp. Thermophys. Properties, NBS Gaithersburg/USA, June 1988
- /15/ Kistler, S.S., Phys. Chem. 46, 19 (1942)
- /16/ Büttner, D., Caps, R., Heinemann, U., Hümmer, E., Kadur, A., Fricke, J., Solar Energy 40, 13 (1988)
- /17/ Broeker, F.J., Heckmann, W., Fischer, F., Mielke, M., Schroeder, J., Stange, A., Structural Analysis of Granular Silica Aerogels in 'Aerogels' Springer Proceedings in Physics 6, Fricke, J. (Ed), Springer Verlag Berlin 1986
- /18/ Kaganer, M.G., Thermal Insulation in Cryogenic Engineering, Jerusalem 1969, Israel Program for Scientific Translations